hydrology

MDPI

Article

Coastal Erosion Caused by River Mouth Migration on a Cuspate Delta: An Example from Thanh Hoa, Vietnam

Dinh Van Duy [1,*], Tran Van Ty [1], Cao Tan Ngoc Than [1], Cu Ngoc Thang [1], Huynh Thi Cam Hong [1], Nguyen Trung Viet [2] and Hitoshi Tanaka [3]

1 Faculty of Water Resource Engineering, College of Engineering, Can Tho University, Can Tho 94115, Vietnam; tvty@ctu.edu.vn (T.V.T.); ctnthan@ctu.edu.vn (C.T.N.T.); cnthang@ctu.edu.vn (C.N.T.); htchong@ctu.edu.vn (H.T.C.H.)
2 Faculty of Civil Engineering, Thuy Loi University, Hanoi 11515, Vietnam; nguyentrungviet@tlu.edu.vn
3 Institute of Liberal Arts and Sciences, Tohoku University, 41 Kawauchi, Aoba-ku, Sendai 980-8576, Japan; hitoshi.tanaka.b7@tohoku.ac.jp
* Correspondence: dvduy@ctu.edu.vn

Abstract: Coastal erosion poses a significant threat to the infrastructure of the coastal community at the mouth of the Ma River in Thanh Hoa Province, Vietnam. In response, emergency solutions such as hard, protective structures are often implemented. However, this approach exacerbates the problem as the underlying mechanisms of coastal erosion are not adequately investigated and understood. In this study, the long-term configuration of the mouth of the Ma River in Thanh Hoa Province, Central Vietnam, is investigated using Landsat imagery spanning from 1987 to 2023. An analytical solution of a one-line model for shoreline change was also used to examine the sand discharge from the Ma River and the diffusion coefficient for the sand transported along the shore by breaking waves. The results showed an asymmetric configuration of the mouth of the Ma River over the past 37 years. The supply of sand from the Ma River is around 350,000 m^3/year. The majority of sand (ranging from 55% to 75%) is mainly transported to the northern beach of the Ma River delta. This uneven distribution of sand from the Ma River has led to the asymmetrical morphology of the delta apex in which the northern part of the Ma River delta is experiencing northward movement while the southern part of the Ma River Delta is moving southward and landward. The asymmetrical morphology of the delta at the mouth of the Ma River has recently been identified as the cause of severe coastal erosion. The diffusion coefficient value determined for the transportation of longshore sand along the deltaic lobes of the Ma River delta corresponds to 90 m^2/day. This study offers a practical method for investigating morphological changes in cuspate deltas, especially when measured field data are limited.

Keywords: coastal erosion; cuspate delta; wave-dominated delta; analytical solution; sediment supply; Landsat; Ma River; Vietnam

Citation: Duy, D.V.; Ty, T.V.; Than, C.T.N.; Thang, C.N.; Hong, H.T.C.; Viet, N.T.; Tanaka, H. Coastal Erosion Caused by River Mouth Migration on a Cuspate Delta: An Example from Thanh Hoa, Vietnam. *Hydrology* **2023**, *10*, 189. https://doi.org/10.3390/hydrology10090189

Academic Editor: Alessio Radice

Received: 1 August 2023
Revised: 3 September 2023
Accepted: 14 September 2023
Published: 18 September 2023

1. Introduction

Cuspate deltas, which were first defined by Wright and Coleman [1], are examples of deltas that protrude slightly into open water. They have been the object of numerous studies by coastal scholars [2–18] because they are one of the three most widely seen delta morphologies classified by Galloway [3]. According to Galloway [3], this type of landform was designated as a wave-dominated delta because the morphologies of these deltas are formed mainly via the interaction between riverine (sediment supply) and ocean (waves) forces.

Due to urbanization and the need for natural resources, 31% of Vietnam's population lives along the coast [19]. However, this narrow coastal belt is susceptible to the threats of waves, flooding, storm surges, and sea level rise [20]. Along the coastline of Vietnam, coastal erosion has become a natural hazard in the last decade and has resulted in significant costs to both communities and nature [21–24].

The Ma River delta is a cuspate delta located in Thanh Hoa Province, Vietnam, as shown in Figure 1. The protruding part of this delta is formed by sediment which was supplied from the Ma River and is under the effects of waves from the Vietnamese East Sea [12]. According to Quang et al. [25], the Ma River delta is the third largest river delta in Vietnam, and it drains 5.17 million tons of sediment into the East Sea annually. Under the action of waves, the sediment supplied from the river is transported along the shore to nourish the beaches on both sides of the mouth of the Ma River. It should be noted that at the end of the southern coast, there is a mountainous region that acts as a boundary to block the further transport of longshore sediment (Figure 1c,d).

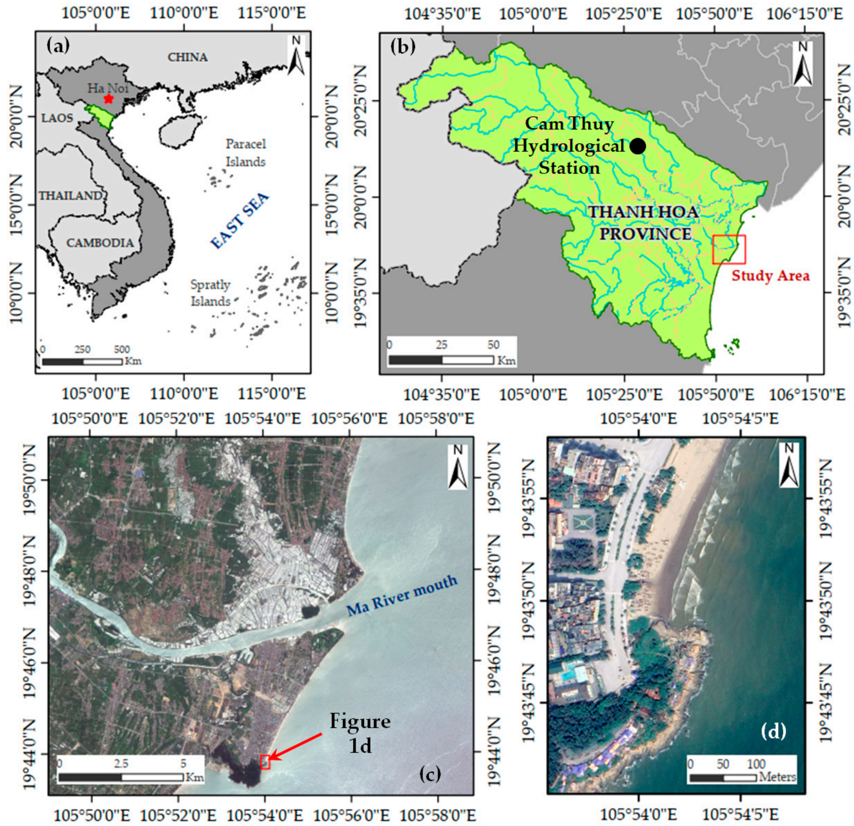

Figure 1. The study area. (**a**) A map of Vietnam; (**b**) Thanh Hoa Province, with the Cam Thuy Hydrological Station located approximately 70 km upstream from the mouth of the Ma River; (**c**) the Ma River delta; (**d**) the mountainous region, which is considered a boundary preventing the transportation of sand.

At the mouth of the Ma River, significant coastal erosion occurs on the cuspate of the delta. Coastal erosion has negatively affected both infrastructures and livelihoods in recent years. The cuspate delta has experienced a significant loss of agricultural land and infrastructure to the sea. Nevertheless, it is evident that numerous coastal areas within Vietnam are characterized by a restricted availability of monitoring data. Consequently, scholars specializing in coastal studies are compelled to utilize methodologies such as numerical models, physical models, or empirical formulas to conduct research, utilizing field observations gathered over a short period [26–29].

To handle the situation of limited data in the Ma River delta, an analytical solution consisting of a one-line model was utilized in combination with a remote-sensing technique to study the long-term evolution of the mouth of the Ma River in Thanh Hoa Province, Vietnam. The relationship between coastal morphological changes and coastal erosion in this cuspate delta were investigated. Based on the idea of the one-line model, this study provides a practical and efficient method of investigating morphological changes in cuspate deltas.

2. Materials and Methods

2.1. Landsat Image Analysis

Landsat imagery has been applied intensively in coastal studies, especially in areas with significant shoreline temporal variations, such as the mouths of rivers, sand spits, and around coastal structures [27,30–34]. In this research, Landsat images spanning the period 1987 to 2023 were gathered (as shown in Table 1) to monitor alterations in the shorelines surrounding the mouth of the Ma River. The images were downloaded annually, with a frequency of one image per year, and only cloud-free images were selected for the study area. Shoreline detection was performed based on the Normalized Difference Water Index (*NDWI*) [35]:

$$NDWI = \frac{X_{green} - X_{nir}}{X_{green} + X_{nir}} \quad (1)$$

where X_{green} and X_{nir} are the GREEN and NIR spectral bands, respectively. Subsequently, the shorelines of several years from 1987 to 2023 were mapped together to observe the temporal variations in the cuspate delta.

Table 1. Information about Landsat images.

No.	Date	Sensor	Resolution (m)	Data Source
1	7 March 1987	TM	30	Landsat 5
2	28 May 1988	TM	30	Landsat 5
3	16 June 1989	TM	30	Landsat 5
4	5 July 1990	TM	30	Landsat 5
5	14 February 1991	TM	30	Landsat 5
6	24 June 1992	TM	30	Landsat 5
7	29 July 1993	TM	30	Landsat 5
8	29 May 1994	TM	30	Landsat 5
9	5 September 1995	TM	30	Landsat 5
10	6 August 1996	TM	30	Landsat 5
11	6 June 1997	TM	30	Landsat 5
12	15 October 1998	TM	30	Landsat 5
13	18 October 1999	TM	30	Landsat 5
14	5 November 2000	TM	30	Landsat 5
15	19 July 2001	TM	30	Landsat 5
16	24 September 2002	TM	30	Landsat 5
17	6 May 2003	TM	30	Landsat 5
18	24 May 2004	TM	30	Landsat 5
19	11 May 2005	TM	30	Landsat 5
20	6 November 2006	TM	30	Landsat 5
21	1 May 2007	TM	30	Landsat 5
22	20 June 2008	TM	30	Landsat 5
23	9 July 2009	TM	30	Landsat 5
24	1 November 2010	TM	30	Landsat 5
25	26 April 2011	TM	30	Landsat 5
26	8 October 2013	OLI/TIRS	30	Landsat 8
27	23 July 2014	OLI/TIRS	30	Landsat 8

Table 1. *Cont.*

No.	Date	Sensor	Resolution (m)	Data Source
28	15 January 2015	OLI/TIRS	30	Landsat 8
29	7 October 2016	OLI/TIRS	30	Landsat 8
30	31 July 2017	OLI/TIRS	30	Landsat 8
31	2 July 2018	OLI/TIRS	30	Landsat 8
32	18 May 2019	OLI/TIRS	30	Landsat 8
33	20 May 2020	OLI/TIRS	30	Landsat 8
34	23 May 2021	OLI/TIRS	30	Landsat 8
35	8 April 2022	OLI/TIRS	30	Landsat 8
36	21 May 2023	OLI/TIRS	30	Landsat 9

2.2. Application of Analytical Solutions for Shoreline Changes

The principle of a one-line model (Figure 2) was used for the analytical approach to understanding the long-term evolution of shoreline changes in the Ma River delta. In the context of the one-line theory, it was assumed that the beach profile retains a balanced form, signifying that all underwater shapes run parallel. As a result of this assumption, a single line can be used to understand shifts in the shoreline. This chosen line conveniently corresponds to the shoreline itself, as illustrated in Figure 2.

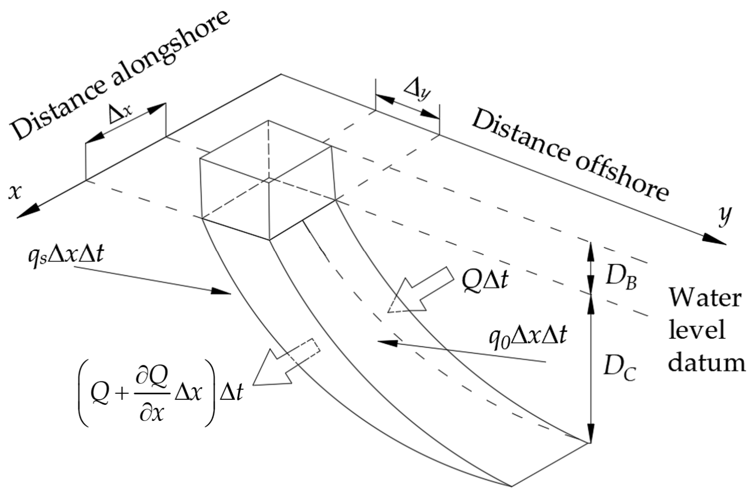

Figure 2. The principle of the one-line model for shoreline change (re-drawn based on the sketch mentioned in Duy et al. [18]).

An analytical solution of a one-line model for shoreline changes in a wave-dominated delta was utilized to quickly estimate the diffusion coefficient for the longshore transport of sand (ε). Currently, there are two types of analytical solutions for modelling the wave-dominated evolution of a river delta. The first solution was introduced by Larson et al. [36] for infinite shorelines (Figure 3a). Later, Duy et al. [18] derived another closed-form solution for shorelines with definite lengths (L) (Figure 3b).

As can be seen in Figure 1d, there is a headland at the end of the southern shoreline in the Ma River delta. This headland can be considered a transport boundary for the further transport of sand, as shown in Figure 3b. Hence, the southern shoreline of the Ma River delta fits the analytical solution proposed by Duy et al. [18] well, as shown below:

$$y = \frac{q_0}{2\varepsilon DL}\left[\frac{x^2}{2} - L|x| + \frac{L^2}{3} + \varepsilon t - \frac{2L^2}{\pi^2}\sum_{n=1}^{\infty}\frac{1}{n^2}e^{-n^2\pi^2\frac{\varepsilon t}{L^2}}\cos\left(\frac{n\pi x}{L}\right)\right] \quad (2)$$

where y is the shoreline position, q_0 is the sand discharged from the river, ε is the diffusion coefficient, D is the sum of the depth of closure (D_C) and the beach berm height (D_B), x is the along-shore distance, and L is the length of the shoreline, which is the distance from the mouth of the river to the rocky boundary. In this study, we considered the rocky boundary in Figure 1d as a no-sand-transport boundary, meaning that it was assumed to prevent the movement of sand along the coastline in the longshore direction. After some time, that portion bounded by the rock will be saturated, resulting in the depletion of sediment from the system. This depletion of sediment offshore is considered a shorterm perturbation and can be ignored in the one-line model.

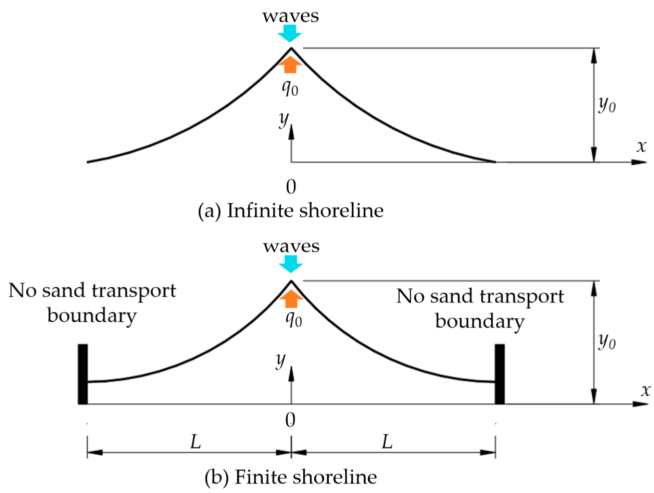

Figure 3. Sketch of river deltas with (**a**) infinite shorelines and (**b**) finite shorelines. The sketch was re-drawn based on the idea of Duy et al. [18]. In this figure, q_0 is the sand supply from the river and y_0 is the maximum extension of the cuspate delta into the ocean.

In order to compare the shoreline extracted from the Landsat images and the shoreline calculated using the analytical solution, a Cartesian coordinate system was used consistently in this study in which the abscissa was 108° counter-clockwise from the north and crossed the point O (595,288.00 m E; 2,188,386.00 m N) in the UTM system (Figure 4b). In the interest of expediency, a 108° counterclockwise rotation was applied to the coordinate system to establish the configuration depicted in Figure 4a.

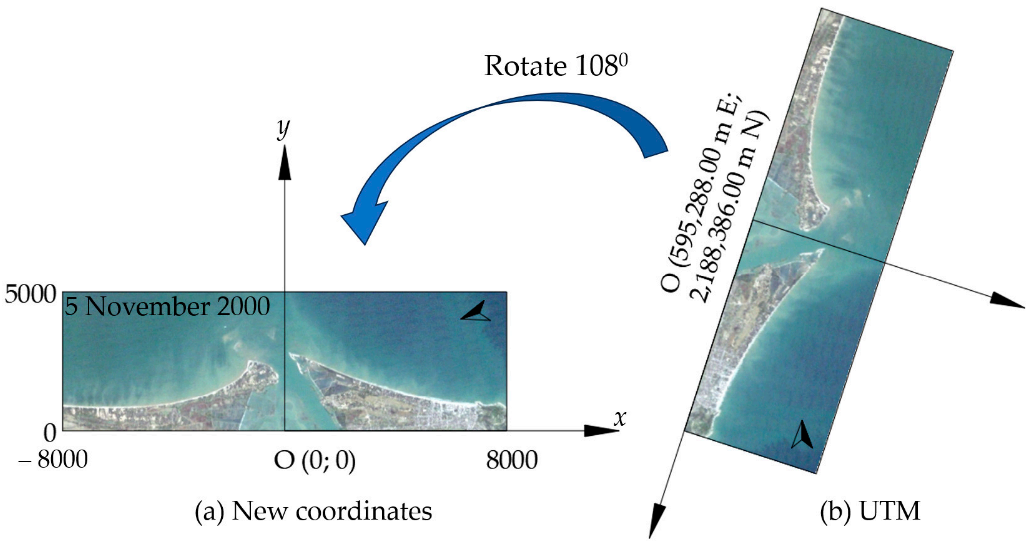

Figure 4. Cartesian coordinates used in this study, achieved by rotating images 108° and taking Origin O (0;0) in Cartesian coordinates as O (595,288.00 m E; 2,188,386.00 m N) in the UTM system.

The shoreline position extracted from the Landsat image obtained on 14 February 1991 was used as the measured data to be compared with the computed data. The shoreline position on 14 February 1991 was chosen since it has the most protruding part of the cuspate delta and a symmetric configuration with respect to the y-axis. These conditions satisfy the shoreline configuration in Figure 3b.

In order to model the shoreline position in 1991 using Equation (2), a comprehensive assembly of the requisite initial variables was undertaken, and their corresponding values are presented in Table 2. The rationale behind the selection of each variable's specific values is expounded upon in subsequent paragraphs.

Table 2. Initial values of variables used for modeling the evolution of the Ma River delta using the analytical solution of Duy et al. [18].

Diffusion Coefficient, ε (m^2/day)	Unknown
Sand supply from the river, q_0 (m^3/year)	390,000
Formation time, t (year)	500
Depth of closure, D_C (m)	5.6
Berm height, D_B (m)	1.8
Length of the shoreline, L (m)	6900

Quang et al. [25], reported that the Ma River discharges a total of 5.17 million tons of sediment annually into the Vietnamese East Sea. Among this amount, 20% constitutes bed load sediment [37]. Consequently, the annual contribution of bed load sediment from the Ma River to the beaches at the mouth of the river is estimated to be $5.17 \times 10^6 \times 20\% = 1.03 \times 10^6$ tons. According to Quang et al. [25], the beaches of the Ma River delta are made of sand. Hence, these beaches are formed mainly via the transportation of bed load sediment from the Ma River. In determining the sand transport rate, considering a sand density of 2650 kg/m^3 [38], the calculated value is

$$q_0 = \frac{1.03 \times 10^6 \times 1000}{2650} = 388,679 \approx 390,000 \left(\mathrm{m}^3/\mathrm{year}\right) \quad (3)$$

This value of q_0 was utilized as the initial value for the supply of sand from the Ma River, as presented in Table 2.

The determination of the formation time (t) draws upon the research conducted by Yen et al. [39]. It is worth noting that while the investigation of Yen et al. [39] focused on the Red River delta, it also included a map encompassing the neighboring Ma River delta. This map provides distinct evidence that the historical shoreline positions in the Late Holocene originated between 500 and 200 years Before Present (BP). Consequently, the time of the establishment of the Ma River delta is considered to be approximately 500 years ago.

The depth of closure was calculated based on the following equation from Hallermeier [40]:

$$D_C = 2.28 H_{se} - 68.5 \left(\frac{H_{se}^2}{g T_{se}^2}\right) \quad (4)$$

where D_C is the depth of closure, H_{se} and T_{se} are the significant wave height and wave period of the extreme wave condition (extremely high waves are expected for 12 h per year), and g is the gravitational acceleration. According to Thomson and Harris [41], T_{se} should be taken to be the typical period of the measured wave height. The extreme high-wave conditions were taken from the study of Hung et al. [42], with H_{se} = 3 m and T_{se} = 7 s, respectively. Substituting H_{se} and T_{se} into Equation (4) yields Dc = 5.6 m.

The beach berm height was calculated based on the expression proposed by Uda [43], as follows:

$$D_B = 0.32 \times D_C \quad (5)$$

The value of Dc = 5.6 m yields D_B = 1.8 m.

Finally, the length of the shoreline was measured from the Landsat image captured on 14 February 1991 as shown in Figure 5.

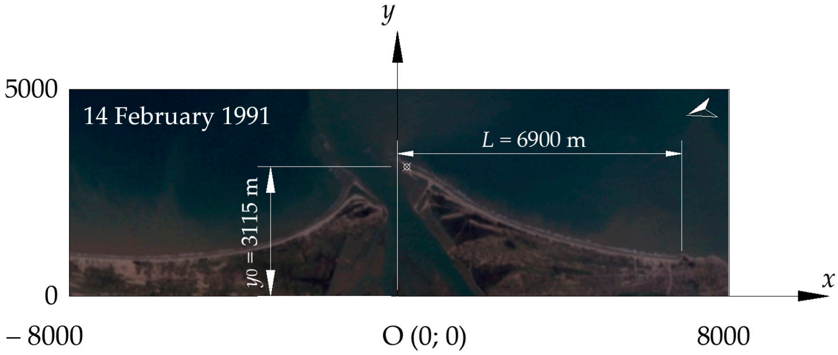

Figure 5. An image of the shoreline configuration captured on 14 February 1991 is compared with the computed shoreline using the analytical solution.

Table 2 contains the initial values employed for computing the shoreline positions in 1991. A comparison between these calculated positions and the shoreline positions extracted from the Landsat image on 14 February 1991 was performed. Given that the value of ε is unknown, an iterative calculation process was adopted, considering a range of ε values. The root mean square error (RMSE) of the shoreline position was utilized to determine the optimal value of ε that best fit the data. Consequently, the iterative process terminated once the minimum RMSE was achieved.

2.3. Geometrical Characteristics of the Cuspate Delta

2.3.1. Evolution of the Cuspate Delta

The along-shore and cross-shore coordinates of the cuspate tips on both sides of the mouth of the Ma River were observed and are used for discussing the morphological behavior of the river's mouth. The method of using the coordinates of special points such as the tips of sand spits or the center of gravity to discuss the evolution of a sand body has been applied widely in coastal engineering [27,30,32,34,44,45]. Figure 6 illustrates the schematic for measuring the coordinates of the cuspate tips, which are considered the most prominent protrusions into the open water. The schematic elucidates the fundamental variables involved in the process, namely x_S and x_N, signifying the along-shore coordinates of the cuspate tips on the southern and northern sectors, respectively. Additionally, the variables y_S and y_N were designated to represent the cross-shore extents of the cuspate tips on the southern and northern parts, respectively. It is imperative to note that all measurements of these variables are expressed in meters.

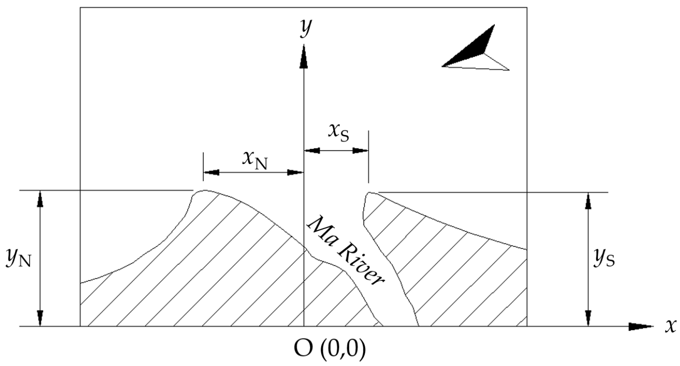

Figure 6. The sketch for measuring the coordinates of the tips on the north (x_N, y_N) and south (x_S, y_S) sectors of the mouth of the Ma River.

2.3.2. Shoreline Orientations at the River Mouth

The investigation of the mouth of the Ma River encompasses not only the geometrical characteristics of the cuspate delta but also the determination of the shoreline orientations. In the context of wave-dominated river deltas, the assessment of the shoreline orientations on both sides of the mouth of the river assumes paramount significance for understanding the evolution of this geographical feature [2,23,46,47]. To facilitate the estimation of shoreline orientations, it is imperative to define shoreline angles. As elucidated in [46], shoreline angles correspond to the angles formed between the trendlines (red lines) and a horizontal reference line, as illustrated in Figure 7. Denoting the shoreline angles on the north and south of the mouth of the Ma River as θ_N and θ_S, respectively, the expressions for the shoreline orientations at the mouth of the river can be represented as follows:

$$\beta_N = \tan(\theta_N) \tag{6}$$

and

$$\beta_S = \tan(\theta_S) \tag{7}$$

where β_N and β_S are the shoreline orientations in the north and the south sections of the river mouth, respectively.

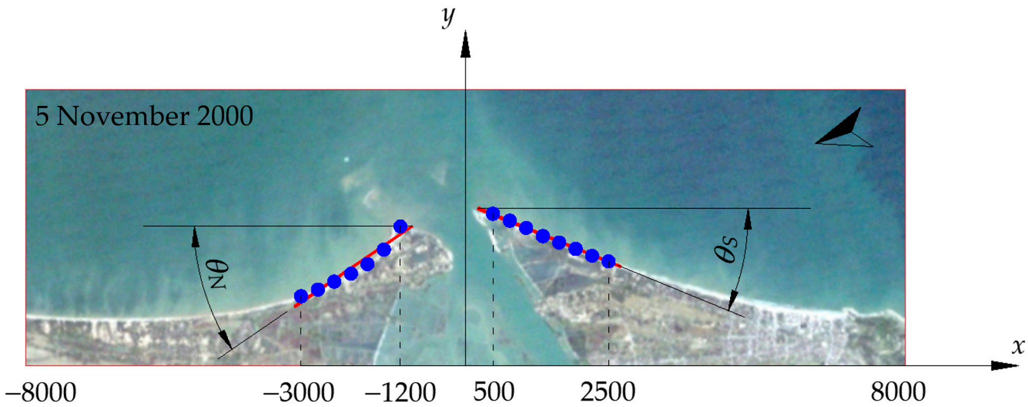

Figure 7. Angles of the cuspate delta on the north (θ_N) and the south (θ_S) sides.

In Figure 7, we examine the angles of the cuspate delta formed in the northern (θ_N) and southern (θ_S) sections. To ascertain the shoreline orientations, we employed a linear regression method, utilizing shoreline positions depicted as blue dots, which were extracted at regular 50 m intervals. For visual clarity, the figure displays shoreline positions at 300 m intervals. The measurement range for the shoreline orientations encompasses -3000 m $\leq x \leq -1200$ m for the northern shoreline and 500 m $\leq x \leq$ 2500 m for the southern shoreline.

According to Hu et al. [48], in wave-dominated river deltas, the shape of the coastline affects the distribution of the sand supplied from the river. This mechanism was also studied by Ashton et al. [49] and Ashton and Giosan [50]. Therefore, it would be useful to investigate the relationship between the shoreline orientations and the rate of the distribution of the sand supplied from the Ma River. If the rate of the distribution of the sand supplied from the Ma River to the north is α, it can be expressed as a function of the shoreline orientations as

$$\alpha = \frac{\beta_N}{\beta_N + \beta_S} \tag{8}$$

3. Results

3.1. Temporal Variations in Shorelines at the River Mouth

The shoreline positions extracted from the Landsat imagery are plotted in Figure 8. Only shoreline positions in 1987, 2000, 2010, and 2023 were plotted to ensure legibility. As can be seen from the figure, the southern tip of the cuspate delta retreated significantly by a distance of approximately 1000 m from 1987 to 2023. On the other hand, the shoreline position of the northern tip moved north.

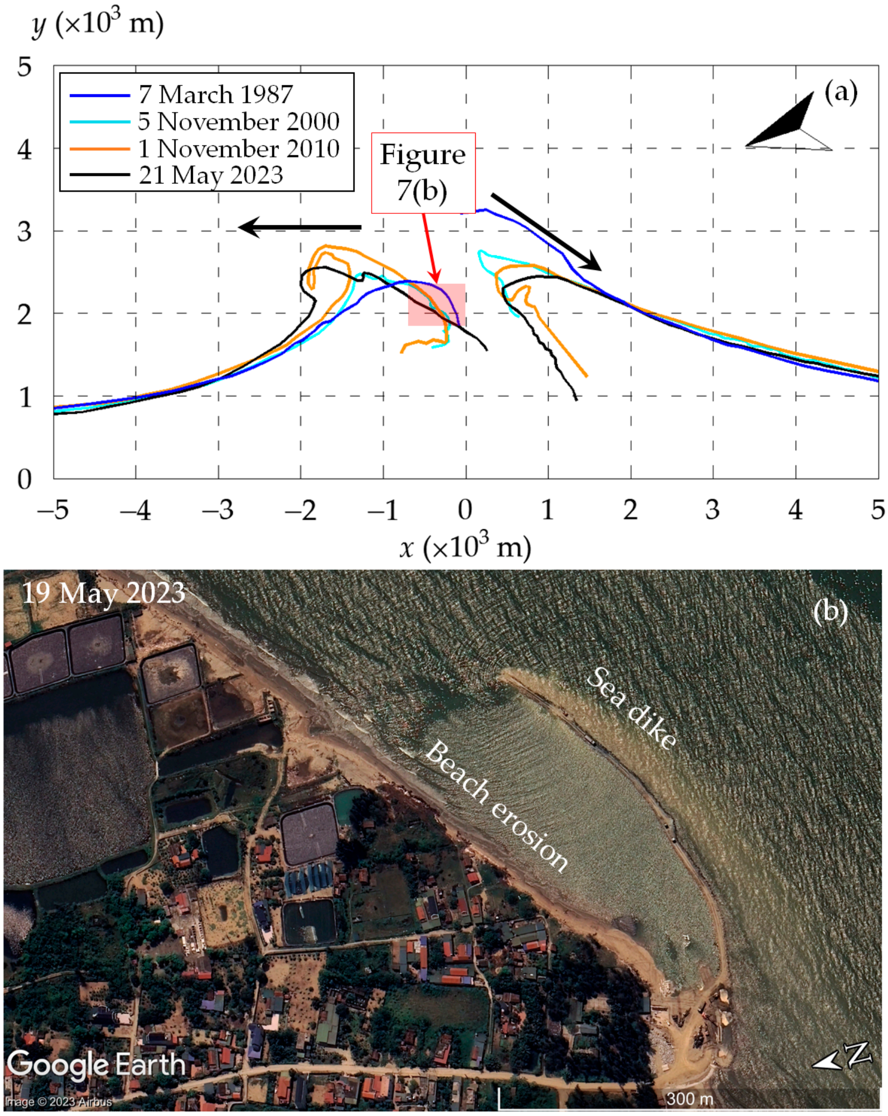

Figure 8. (**a**) Temporal variations in shorelines at the mouth of the Ma River. (**b**) Beach erosion due to the northward shifting of the river mouth; a sea dike was built by the local government to reduce wave forces prior to the construction of an embankment to prevent coastal erosion (image downloaded from Google Earth™).

Moreover, a significant northward displacement of the shoreline at the erosion hotspot (indicated by the red rectangle in Figure 8a) was also observed, measuring a distance of approximately 200 m. These shifting shoreline patterns are attributed to severe coastal erosion, which has prompted local communities to implement the use of hard structures as a protective measure, as illustrated in Figure 8b.

3.2. Diffusion Coefficient for Sand Transport Induced by Breaking Waves

Figure 9 displays the optimal alignment between the computed shoreline and the observed shoreline. In this context, the shoreline position in 1991, determined through Equation (2), is depicted by a red line, while the shoreline position obtained from the Landsat image taken on 14 February 1991 is represented by blue dots (the measured shoreline). The minimum root mean square error (RMSE) between these shoreline positions amounts to 26.4 m. For reference, Table 3 presents the final values of the variables employed in the calculation procedure.

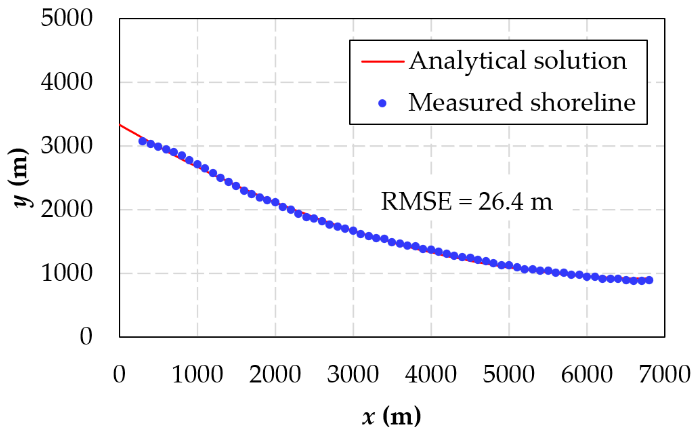

Figure 9. Comparison between the computed shoreline and the measured shoreline in 1991.

Table 3. The final values of the variables used for modeling the evolution of the Ma River delta, using the analytical solution of Duy et al. [18].

Diffusion coefficient, ε (m^2/day)	90
Sand supply from the river, q_0 (m^3/year)	350,000
Formation time, t (year)	500
Depth of closure, D_C (m)	5.6
Berm height, D_B (m)	1.8
Length of the shoreline, L (m)	6900

3.3. Geometrical Characteristics of the Cuspate Delta

3.3.1. Evolution of the Cuspate Delta

Figure 10 shows the long-term variations in the coordinates of the northern and southern sand cuspate tips over time in the along-shore direction. The horizontal axis represents the timeline, ranging from 1987 to 2023. The vertical axis represents the along-shore coordinates of the evolution of the cuspate tips, measured in meters. The blue circles on the graph represent the along-shore coordinate for the southern cuspate tip (x_S), while the orange squares represent the along-shore coordinate for the northern cuspate tip (x_N).

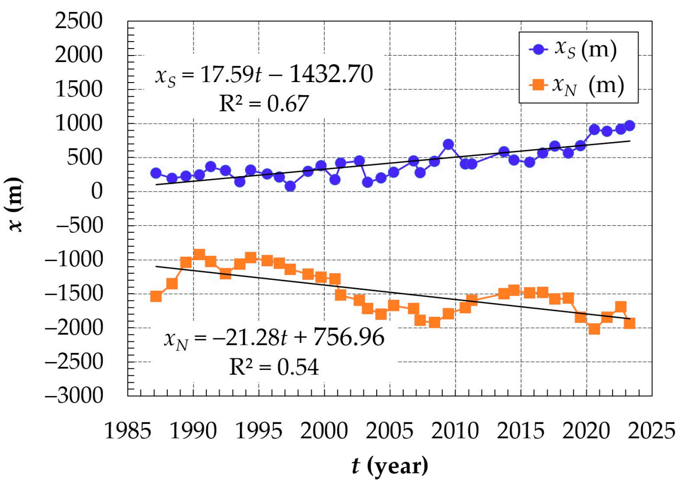

Figure 10. Temporal variation in the coordinates of the northern and southern cuspate tips in the along-shore direction.

From the data presented in Figure 10, it is evident that both cuspate tips have been moving in opposite directions along the shoreline over time. The southern cuspate tip (x_S) has shown an increasing trend, moving at a rate of 17.59 m per year to the south. On the other hand, the northern cuspate tip (x_N) has been decreasing in its along-shore coordinate, moving at a rate of approximately −21.28 m per year to the north. These observations are in line with the changes observed in the shoreline of the mouth of the Ma River, as depicted in Figure 8a.

Figure 11 presents a diagram of the temporal variations in the cuspate tips in the cross-shore direction from 1987 to 2023. The diagram includes two sets of data points represented by different shapes and colors. The orange triangles represent the coordinates of the southern cuspate tip (y_S), while the blue diamonds represent the northern cuspate tip (y_N).

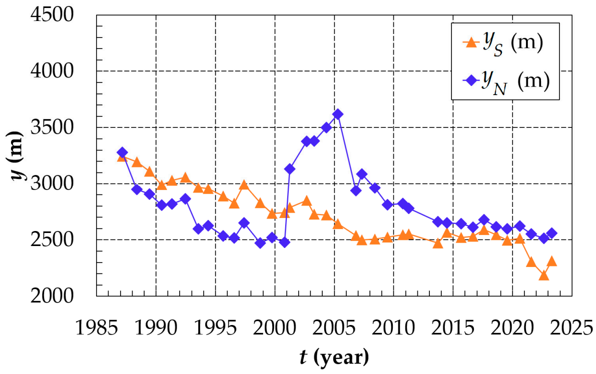

Figure 11. Temporal variations in the coordinates of the northern and southern cuspate tips in the cross-shore direction.

Concerning the southern cuspate tip, the cross-shore coordinate of the southern cuspate tip decreased steadily over the tracking time. This means that the position of the southern cuspate tip moved closer to the shoreline as time progressed.

On the other hand, the cross-shore coordinates of the northern cuspate tip showed fluctuations during the survey period. From 1987 to 2000, the northern cuspate tip's cross-shore coordinate decreased. This indicates that the position of the northern cuspate tip moved closer to the shoreline during this time period. Between 2001 and 2005, there was a sharp increase in the northern cuspate tip's cross-shore coordinate. It expanded from 2000 m to 3600 m, indicating that the northern cuspate tip moved further away from the shoreline during this period. Since 2006, the northern cuspate tip's cross-shore coordinate decreased significantly and has reached 2500 m again as of the time of writing. This suggests that the position of the northern cuspate tip moved closer to the shoreline again in recent years.

In addition, the significant increase in the northern cuspate tip's cross-shore coordinate from 2001 to 2005 indicates a large sediment supply from the Ma River, but the protrusion towards the sea of only the northern cuspate tip implies an asymmetric distribution of this sand supply, favoring the northern cuspate tip.

3.3.2. Shoreline Orientations at the River Mouth

Figure 12 illustrates the temporal variation in the shoreline orientations at the mouth of the Ma River. The diagram displays two key values: β_N, representing the shoreline orientation in the north, and β_S, representing the shoreline orientation in the south.

The diagram indicates that there is a significant gap between the shoreline orientations of the north and the south. This disparity suggests that the cuspate delta in the Ma River possesses an asymmetric shape. In other words, the two sides of the river mouth, the northern and southern tips, have different angles at which they meet the water.

Furthermore, the higher values of β_N compared to the values of β_S indicate that the northern tip of the river mouth protrudes more prominently into the water than the southern one. This difference in protrusion further contributes to the overall asymmetry of the cuspate delta.

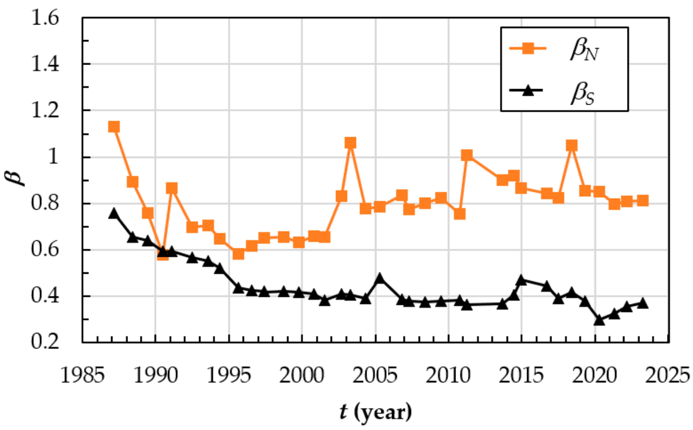

Figure 12. Shoreline orientations on both sides of the mouth of the river.

Figure 13 illustrates the calculated ratio of sand supplied to the northern lobe of the Ma River delta from 1987 to 2023. The ratio was determined using Equation (8), and the results indicate that the amount of sand supplied to the northern lobe has consistently been larger than the amount of sand supplied to the southern lobe during this period. The trend over time shows a continuous increase in the sand supplied to the northern lobe, indicating a greater deposition of sand in that region compared to the south. This is evidenced by all the data points consistently lying above the midpoint (α = 0.5), suggesting an asymmetric distribution of sand towards the north (from 55% to 75%). However, there was an exception in the year 1990, when the sand supply was equal on both sides of the mouth of the Ma River, resulting in a balanced ratio with a value of α equal to 0.5. This suggests that in 1990, the distribution of sediment between the northern and southern lobes was approximately equal.

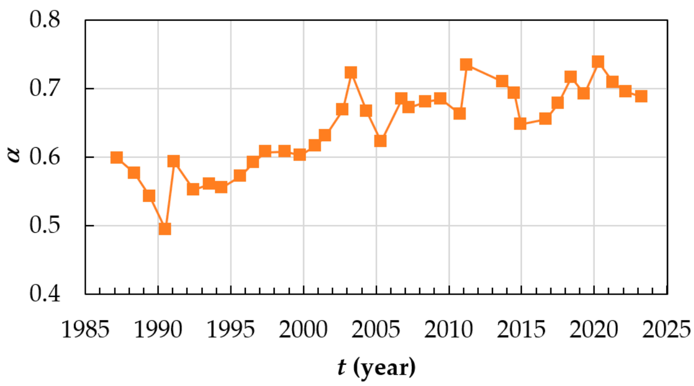

Figure 13. Ratio of sand supplied to the north.

4. Discussion

The daily suspended sediment concentration (R) measured at the Cam Thuy Hydrological Station is plotted with the evolution of the coordinates of the southern tip in the cross-shore direction in Figure 14. It can be noted that the values of R were only measured from 2004. It can be seen from the figure that the significant values of R in 2004 and 2005 correspond to the sudden seaward transition of the northern tip between 2004 and 2005.

Figure 15 shows a representation of a river mouth in which sand is being supplied symmetrically to both sides of the river's opening. Additionally, the sketch includes illustrations of longshore sand transport along the coastlines. Arrows are drawn parallel to the shorelines, indicating the direction of the movement of sand along the coast.

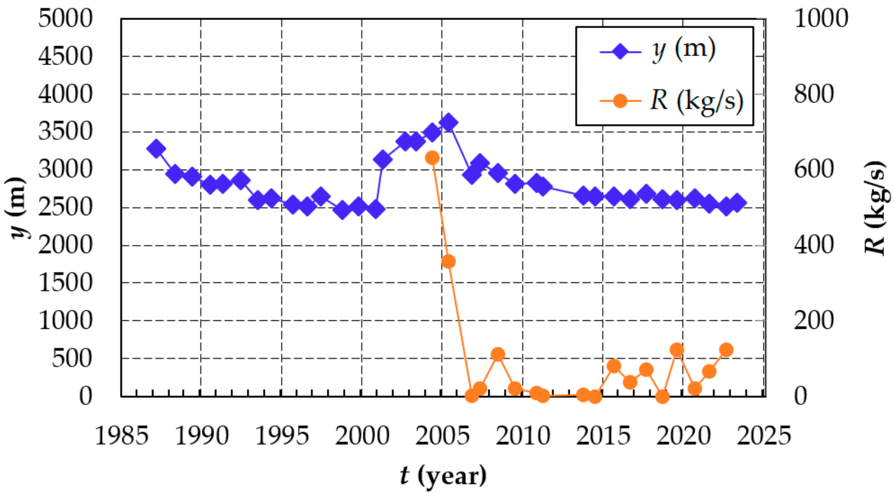

Figure 14. The relationship between the concentration of suspended sediment and the coordinate of the southern tip in the cross-shore direction.

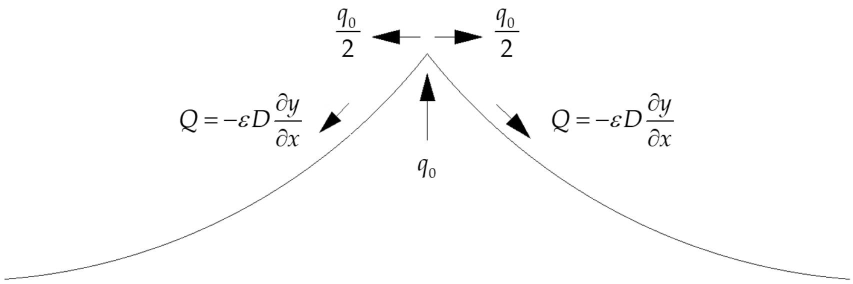

Figure 15. Symmetric sand distribution at the mouth of the river and the rate of along-shore sand transport.

According to the study by Duy et al. [18], longshore sand transport can be mathematically expressed as

$$Q = -\varepsilon D \frac{\partial y}{\partial x} \tag{9}$$

where Q is the longshore transport of sand along the coastline, and $\frac{\partial y}{\partial x}$ is the shoreline's orientations at the river mouth; $\frac{\partial y}{\partial x} = \tan\theta = \beta$.

By equating Q and $q_0/2$, we obtain

$$\frac{\partial y}{\partial x} = -\frac{q_0}{2\varepsilon D} \tag{10}$$

For the asymmetric condition at the Ma River delta, the sand supply from the Ma River and the ratios of the sand transported to the north and south at the mouth of the Ma River can be calculated as follows:

- Sand supply from the Ma River:

$$q_0 = (\beta_N + \beta_S)\varepsilon D \tag{11}$$

- Sand transported to the north:

$$q_N = \alpha q_0 \tag{12}$$

- Sand transported to the south:

$$q_S = (1-\alpha) q_0 \tag{13}$$

Figure 16 shows the sand supplied from the Ma River (orange squares) and the amounts of sand distributed to the north (blue diamonds) and the south (black dots), respectively. There is an asymmetric distribution of sand to the north and the south of the delta which indicates that the waves approach the delta from a dominant direction more often at this study site. This phenomenon can be explained by considering the wind fetch lengths, which can be observed in Figure 1a. Figure 1a distinctly reveals a pronounced disparity in fetch length between the prevailing S and SE wind directions in comparison to the NW, N, and NE sectors. As a result, it can be inferred that wave perturbations originating from the S/SE sectors are likely to induce significant longshore currents that are directed towards the NW direction and lead to the asymmetric configuration of the delta tip.

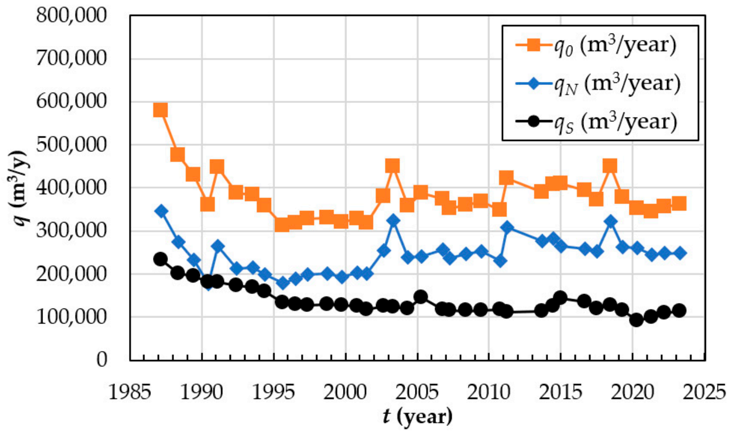

Figure 16. Temporal variations of sediment supplied from the Ma River.

In Figure 16, it is interesting that the average amount of sand supplied by the Ma River is around 380,000 m^3/year. This value is very close to the sand supply estimated using the analytical solution shown in Table 3 (350,000 m^3/year).

5. Conclusions

Coastal erosion at the mouth of the Ma River in Thanh Hoa Province, Vietnam, was investigated using Landsat imagery from 1987 to 2023 and via analytical means. The research findings reveal the following key points:

- The northern part of the Ma River delta has experienced northward movement, leading to severe coastal erosion at the mouth of the river.
- In contrast, the southern part of the Ma River Delta has been moving southward and landward.
- The sand diffusion coefficient at the Ma River delta was calculated to be 90 m^2/day, indicating the rate at which sand particles are transported.
- The present investigation provides an evaluation of the supply of sand originating from the Ma River to the delta's lobes. According to the analytical solution, the estimated annual sand supply amounts to approximately 350,000 m^3/year. Additionally, an alternative approach based on the shoreline orientations at the mouth of the river yields a slightly higher value of approximately 380,000 m^3/year. This discrepancy underscores the reliability of the sand supply assessment derived through the methodologies utilized.
- The research also highlights the asymmetric configuration of the shapes of the shoreline at the mouth of the Ma River, as seen in the uneven distribution of sediment to the delta flanks in which the ratio of sand supplied to the north ranges from 55% to 75%.

The results of this study offer significant contributions to the understanding of the coastal erosion dynamics observed at the estuary of the Ma River. These findings offer insights towards establishing prospective strategies for the coastal zone which may encompass interventions such as the implementation of jetties and harbors. Nevertheless, it is essential that antecedent to the construction of any coastal infrastructures, comprehensive research endeavors are undertaken to mitigate and attenuate any potential adverse ramifications that such constructions might impart upon the delicate coastal ecosystem [51,52].

In the absence of a cross-shore beach profile along the Ma River delta's lobes, as well as the water level measured at the mouth of the river, this study was conducted without taking into account the tidal correction for the shoreline positions. Therefore, care must be taken when using the results of this investigation.

Author Contributions: Conceptualization, H.T. and D.V.D.; methodology, H.T. and D.V.D.; formal analysis, D.V.D., C.T.N.T., C.N.T. and H.T.C.H.; investigation, D.V.D., C.T.N.T. and H.T.C.H.; resources, D.V.D., H.T. and C.N.T.; data curation, H.T. and D.V.D.; writing—original draft preparation, D.V.D., H.T. and T.V.T.; writing—review and editing, H.T., N.T.V., T.V.T. and D.V.D.; visualization, H.T. and D.V.D.; supervision, H.T., N.T.V. and T.V.T.; funding acquisition, H.T. and T.V.T. All authors have read and agreed to the published version of the manuscript.

Funding: This research received no external funding.

Data Availability Statement: Datasets utilized in this study are contained within the article. Further data requests should be addressed to the corresponding author.

Conflicts of Interest: The authors declare no conflict of interest.

References

1. Wright, L.D.; Coleman, J.M. Variations in Morphology of Major River Deltas as Functions of Ocean Wave and River Discharge Regimes. *AAPG Bull.* **1973**, *57*, 370–398. [CrossRef]
2. Komar, P.D. Computer models of delta growth due to sediment input from rivers and longshore transport. *Geol. Soc. Am. Bull.* **1973**, *84*, 2217–2226. [CrossRef]
3. Galloway, W.E. *Process Framework for Describing the Morphologic and Stratigraphic Evolution of Deltaic Depositional Systems*; Datapages, Inc.: Tulsa, OK, USA, 1975.
4. Pranzini, E. A model for cuspate delta erosion. In *Waterfront Planning and Development*; ASCE: Reston, VA, USA, 1989; pp. 4345–4357.
5. Refaat, H.E.-d.A.A. The Formation and Reduction Processes of River Deltas and Their Control. Ph.D. Thesis, Kyoto University, Kyoto, Japan, 1990.
6. Mikhailova, M. Sediment balance in nontidal river mouths and method of calculation of protruding delta formation. *Water Resour (Vodn. Resur.)* **1995**, *5*, 502–510.
7. Pranzini, E. Updrift river mouth migration on cuspate deltas: Two examples from the coast of Tuscany (Italy). *Geomorphology* **2001**, *38*, 125–132. [CrossRef]
8. Bhattacharya, J.P.; Giosan, L. Wave-influenced deltas: Geomorphological implications for facies reconstruction. *Sedimentology* **2003**, *50*, 187–210. [CrossRef]
9. Mikhailova, M. Quantitative assessment of the role of deltas in the processes of deposition of river sediments. *Water Resour.* **2007**, *34*, 644–656. [CrossRef]
10. Seybold, H.; Andrade, J.S., Jr.; Herrmann, H.J. Modeling river delta formation. *Proc. Natl. Acad. Sci. USA* **2007**, *104*, 16804–16809. [CrossRef]
11. Nienhuis, J.H. Plan-View Evolution of Wave-Dominated Deltas. Ph.D. Thesis, Massachusetts Institute of Technology, Cambridge, MA, USA, 2016.
12. Quan, N.C.; Hung, P.V. Characteristics of dynamic geomorphology of coastal-river mouth zones of Ma river, Thanh Hoa province. *Vietnam J. Earth Sci.* **2016**, *38*, 59–65.
13. Besset, M.; Anthony, E.J.; Sabatier, F. River delta shoreline reworking and erosion in the Mediterranean and Black Seas: The potential roles of fluvial sediment starvation and other factors. *Elem. Sci. Anthr.* **2017**, *5*, 54. [CrossRef]
14. Tuan, N.Q.; Tin, H.C.; Quang, L.; Tuan, T.A. Historical Monitoring of Shoreline Changes in the Cua Dai Estuary, Central Vietnam Using Multi-Temporal Remote Sensing Data. *Geosciences* **2017**, *7*, 72. [CrossRef]
15. Anthony, E.J.; Besset, M.; Zainescu, F.; Sabatier, F. Multi-Decadal Deltaic Land-Surface Changes: Gauging the Vulnerability of a Selection of Mediterranean and Black Sea River Deltas. *J. Mar. Sci. Eng.* **2021**, *9*, 512. [CrossRef]
16. Quang, D.N.; Ngan, V.H.; Tam, H.S.; Viet, N.T.; Tinh, N.X.; Tanaka, H. Long-Term Shoreline Evolution Using DSAS Technique: A Case Study of Quang Nam Province, Vietnam. *J. Mar. Sci. Eng.* **2021**, *9*, 1124. [CrossRef]
17. Broaddus, C.M.; Vulis, L.M.; Nienhuis, J.H.; Tejedor, A.; Brown, J.; Foufoula-Georgiou, E.; Edmonds, D.A. First-Order River Delta Morphology Is Explained by the Sediment Flux Balance from Rivers, Waves, and Tides. *Geophys. Res. Lett.* **2022**, *49*, e2022GL100355. [CrossRef]
18. Duy, D.V.; Tanaka, H.; Larson, M.; Viet, N.T. A Theory for Estuarine Delta Formation with Finite Beach Length under Sediment Supplied from the River. *J. Mar. Sci. Eng.* **2022**, *10*, 947. [CrossRef]

19. Lappe, R.; Ullmann, T.; Bachofer, F. State of the Vietnamese Coast—Assessing Three Decades (1986 to 2021) of Coastline Dynamics Using the Landsat Archive. *Remote Sens.* **2022**, *14*, 2476.
20. Ghiasian, M.; Carrick, J.; Rhode-Barbarigos, L.; Haus, B.; Baker, A.C.; Lirman, D. Dissipation of wave energy by a hybrid artificial reef in a wave simulator: Implications for coastal resilience and shoreline protection. *Limnol. Oceanogr. Methods* **2021**, *19*, 1–7. [CrossRef]
21. Duc, D.M.; Nhuan, M.T.; Ngoi, C.V. An analysis of coastal erosion in the tropical rapid accretion delta of the Red River, Vietnam. *J. Asian Earth Sci.* **2012**, *43*, 98–109. [CrossRef]
22. Anthony, E.J.; Brunier, G.; Besset, M.; Goichot, M.; Dussouillez, P.; Nguyen, V.L. Linking rapid erosion of the Mekong River delta to human activities. *Sci. Rep.* **2015**, *5*, 14745. [CrossRef] [PubMed]
23. Tanaka, H.; Viet, N.T.; Hoang, V.C.; Duy, D.V. Erosion mechanism of Cua Dai Beach, Central Vietnam. *J. Jpn. Soc. Civ. Eng. Ser. B3 (Ocean Eng.)* **2015**, *71*, I_449–I_454. [CrossRef]
24. Fan, D.; Nguyen, D.V.; Su, J.; Bui, V.V.; Tran, D.L. Coastal morphological changes in the Red River Delta under increasing natural and anthropic stresses. *Anthr. Coasts* **2019**, *2*, 51–71. [CrossRef]
25. Nguyen, M.Q.; Vu, V.H.; Mai, T.T.; To, X.B.; Tran, N.D.; Dang, M.T.; Dang, X.T.; Nguyen, T.M.; Hoang, V.T.; Giap, T.K.C. Geomorphological sedimentary characteristics in the coastal area of Ma river delta, Thanh Hoa province. *Vietnam J. Mar. Sci. Technol.* **2021**, *21*, 283–298. [CrossRef]
26. Do, A.T.K.; Kralli, V.E.; De Vries, S.; Nguyen, V.T.; Stive, M.J.F. Morphodynamics of a Seasonal Inlet: A Case Study Using Remote Sensing and Numerical Modelling for Cua Dai Inlet, Central Vietnam. In Proceedings of the APAC 2019, Singapore, 20–22 June 2019; Springer: Singapore, 2020; pp. 417–425.
27. Duc Anh, N.Q.; Tanaka, H.; Tam, H.S.; Tinh, N.X.; Tung, T.T.; Viet, N.T. Comprehensive Study of the Sand Spit Evolution at Tidal Inlets in the Central Coast of Vietnam. *J. Mar. Sci. Eng.* **2020**, *8*, 722. [CrossRef]
28. Nguyen, N.-M.; Van, D.D.; Le, D.T.; Cong, S.D.; Pham, N.T.; Nguyen, Q.; Tran, B.; Wright, D.P.; Tanim, A.H.; Anh, D.T. Wave reduction efficiency for three classes of breakwaters on the coastal Mekong Delta. *Appl. Ocean Res.* **2022**, *129*, 103362. [CrossRef]
29. Zemann, M.; van der Linden, R.; Trinh Cong, D.; Vu, D.H.T.; Nguyen, N.M.; Seidel, F.; Oberle, P.; Nestmann, F.; Fink, A.H. Modelling ocean wave conditions at a shallow coast under scarce data availability—A case study at the western coast of the Mekong Delta, Vietnam. *EGUsphere* **2023**, *2023*, 1–22. [CrossRef]
30. Tanaka, H.; Hoang, V.C.; Viet, N.T. Investigation of morphological change at the Cua Dai river mouth through satellite image analysis. *Coast. Eng. Proc.* **2016**, *1*, sediment.9. [CrossRef]
31. Hein, C.J.; Fallon, A.R.; Rosen, P.; Hoagland, P.; Georgiou, I.Y.; FitzGerald, D.M.; Morris, M.; Baker, S.; Marino, G.B.; Fitzsimons, G. Shoreline dynamics along a developed river mouth barrier island: Multi-decadal cycles of erosion and event-driven mitigation. *Front. Earth Sci.* **2019**, *7*, 103. [CrossRef]
32. Lawson, S.K.; Tanaka, H.; Udo, K.; Hiep, N.T.; Tinh, N.X. Morphodynamics and Evolution of Estuarine Sandspits along the Bight of Benin Coast, West Africa. *Water* **2021**, *13*, 2977. [CrossRef]
33. Carvalho, B.C.; Gomes, C.L.d.S.; Guerra, J.V. Spatio-temporal morphological variability of a tropical barrier island derived from the Landsat collection. *Front. Remote Sens.* **2023**, *4*, 1111696. [CrossRef]
34. Duy, D.V.; Ty, T.V.; Thanh, T.N.; Minh, H.V.T.; De, C.V.; Duong, V.H.T.; Dan, T.C.; Viet, N.T.; Tanaka, H. Sand Spit Morphology at an Inlet on Phu Quoc Island, Vietnam. *Water* **2023**, *15*, 1941. [CrossRef]
35. McFeeters, S.K. The use of the Normalized Difference Water Index (NDWI) in the delineation of open water features. *Int. J. Remote Sens.* **1996**, *17*, 1425–1432. [CrossRef]
36. Larson, M.; Hanson, H.; Kraus, N.C. *Analytical Solutions of the One-Line Model of Shoreline Change*; Coastal Engineering Research Center: Vicksburg, MS, USA, 1987.
37. World Bank. *Vietnam—Trung Son Hydropower Project: Environmental Assessment (Vol. 7): Supplementary Environmental and Social Impact Assessment (English)*; World Bank Group: Washington, DC, USA, 2009.
38. Rosati, J.D.; Walton, T.; Bodge, K. Longshore Sediment Transport. In *Coastal Engineering Manual*; U.S. Army Corps of Engineers: Washington, DC, USA, 2002; p. 119.
39. Yen, H.P.H.; Nhan, T.T.T.; Nghi, T.; Toan, N.Q.; Khien, H.A.; Lam, D.D.; Van Long, H.; Thanh, D.X.; Hung, N.T.; Trang, N.T.H.; et al. Late Pleistocene-Holocene sedimentary evolution in the coastal zone of the Red River Delta. *Heliyon* **2021**, *7*, e05872. [CrossRef] [PubMed]
40. Hallermeier, R.J. Uses for a calculated limit depth to beach erosion. In *Coastal Engineering 1978*; Amer Society of Civil Engineers: Reston, VA, USA, 1978; pp. 1493–1512.
41. Thompson, E.F.; Harris, D.L. A Wave CI imatology for US Coastal Waters. In Proceedings of the Offshore Technology Conference, Houston, TX, USA, 1–3 May 1972; OnePetro: Richardson, TX, USA, 1972.
42. Thanh, H.N.; Cuong, V.D.; Tajima, Y.; Cuong, T.V. Numerical modeling of Hydrodynamics and sediment transport processes in Ma rivier estuary, Vietnam. In Proceedings of the 19th IAHR-APD Congress, Hanoi, Vietnam, 21–24 September 2014.
43. Uda, T. *Japan's Beach Erosion: Reality and Future Measures*; World Scientific: Singapore, 2010.
44. Duy, D.V.; Tanaka, H.; Mitobe, Y.; Duc Anh, N.Q.; Viet, N.T. Sand Spit Elongation and Sediment Balance at Cua Lo Inlet in Central Vietnam. *J. Coast. Res.* **2018**, *81*, 32–39. [CrossRef]
45. Paladio-Hernandez, A.; Salles, P.; Arriaga, J.; López-González, J. Characterization of the Morphological Behavior of a Sand Spit Using UAVs. *J. Mar. Sci. Eng.* **2022**, *10*, 600. [CrossRef]

46. Furuike, K.; Uda, T.; Serizawa, M.; San-nami, T.; Ishikawa, T. Model for predicting long-term beach changes originating from accretive features of a natural delta coast. In *Asian and Pacific Coasts 2009: (In 4 Volumes, with CD-ROM)*; World Scientific: Singapore, 2010; pp. 266–272.
47. Uda, T.; Shiho, M.; Toshiro, S.-N.; Masumi, S. A Long-Term Prediction of Beach Changes around River Delta using Contour-Line-Change Model. In *Sedimentary Processes*; Gemma, A., Ed.; IntechOpen: Rijeka, Croatia, 2019; p. Ch. 5. [CrossRef]
48. Hu, N.; Murray, A.B.; Ratliff, K.M.; Little, Z.; Hutton, E.W.H. Wave-Climate Asymmetry Influence on Delta Evolution and River Dynamics. *Geophys. Res. Lett.* **2022**, *49*, e2021GL096315. [CrossRef]
49. Ashton, A.; Murray, A.B.; Arnoult, O. Formation of coastline features by large-scale instabilities induced by high-angle waves. *Nature* **2001**, *414*, 296–300. [CrossRef]
50. Ashton, A.D.; Giosan, L. Wave-angle control of delta evolution. *Geophys. Res. Lett.* **2011**, *38*. [CrossRef]
51. Gao, J.; Ma, X.; Dong, G.; Chen, H.; Liu, Q.; Zang, J. Investigation on the effects of Bragg reflection on harbor oscillations. *Coast. Eng.* **2021**, *170*, 103977. [CrossRef]
52. Gao, J.; Shi, H.; Zang, J.; Liu, Y. Mechanism analysis on the mitigation of harbor resonance by periodic undulating topography. *Ocean Eng.* **2023**, *281*, 114923. [CrossRef]